JOURNAL OF SPACECRAFT AND ROCKETS
Vol. 40, No. 4, July–August 2003

Diffusion and Chemical Reaction by the Finite Element Method

D. T. Wadiak*
Lockheed Martin Space Systems Company, Sunnyvale, California 94088
and
T. K. Hight†
University of Santa Clara, Santa Clara, California 95053-0602

The method of modifying the differential equations describing the diffusion and chemical reaction in solids for solution by the finite element (FE) method to simulate chemical aging in polymers is described. The purpose is to predict chemical aging process in solid polymers. Henry's law is applied to modify the mass balance equations to meet the requirement of an FE continuous solution variable at the material, and the resulting mass balance equations' analogy with the heat conduction equation is exploited to utilize existing FE coding. The FE architecture formulations for the solution vector, stiffness, and capacitance matrices for simple one-dimensional solid parametric elements are presented. The ability of the method to compute a numerical solution that preserves discontinuities in chemical species concentration at dissimilar material interfaces is described and illustrated. The method is extended to include temperature effects by coupling the heat conduction equation to the FE solution of the mass balance equations. An application is presented, the chemical aging of large assets. Aging data are presented in a comparison to model predictions. A single set of material properties and boundary conditions were found that fit the chemical profile data for the two assets of different ages.

Nomenclature

A	=	one-dimensional bar element cross-sectional area, cm^2
C_i	=	mass concentration of the ith species, g/cm^3
C_p	=	heat capacity, cal/g $\cdot$ °C
D_i	=	diffusivity of the ith species, cm^2/s
D_0, S_0, k_0	=	Arrhenius preexponentials
E	=	activation energy, kcal/g $\cdot$ mole $\cdot$ K
$\boldsymbol{j}_i$	=	ith species mass flux, g/cm^2 $\cdot$ s
k	=	reaction rate constants
k_j	=	reaction rate constants for species r through s participating in the rate expression in Eq. (5), g/cm^3 $\cdot$ s
n	=	individual reaction orders in Eq. (5)
$\boldsymbol{n}$	=	unit normal vector at the element external surface
p_i	=	species i partial pressure in the gas phase above the mixture, atm
R	=	universal gas constant
R_i	=	volumetric rate of chemical reaction of the ith species, g/cm^3 $\cdot$ s
S_i	=	species i solubility, g/cm^3 $\cdot$ atm
T	=	temperature, °C
$\boldsymbol{T}$	=	temperature vector, °C
t	=	time, s
$\boldsymbol{u}$	=	displacement vector
X	=	thickness, arbitrary units
Γ	=	external boundary of the computational domain
κ	=	heat conductivity, cal/cm $\cdot$ s
ρ	=	mass density, g/cm^3
Φ	=	volumetric heat rate, cal/cm^3 $\cdot$ s

Received 2 March 2002; revision received 25 August 2002; accepted for publication 10 September 2002.

*Staff Research Engineer, Missile Systems Operations, Propulsion and Controls, O/83-02 B157, 1111 Lockheed Martin Way; also Ph.D. Candidate, Department of Mechanical Engineering, University of Santa Clara, Santa Clara, CA 95053-0602.

†Associate Professor, Department of Mechanical Engineering, 500 El Camino Real.

Introduction

MANY materials in engineering applications eventually suffer from chemical degradation over time that renders them unfit for service. Our daily lives are full of instances ranging from appliances, automobiles, and electronics to, even, paper. In many instances, when a product reaches the end of its useful life, it is repaired or replaced. However, the nature of some products, or their service environment, makes it difficult or prohibitively costly to repair or replace them, such as satellites, spacecraft, or strategic weapons. These products are required to operate, or expected to perform or be stored over long periods and are expected to operate within strict limits at any time during a long service life.[1–7]

When product reliability and long life are paramount, or repair and/or replacement is very costly or very difficult, then aging effects become critical to understand and predict with confidence. The motivation for using a prediction method based on the internal aging processes is that, if successful, it promises to provide more accurate assessments of future states if all relevant aging processes are embodied in the solutions to the governing equations. The cost of this approach over the more common approach of curve fitting is that usually more data are required to provide the material parameters, environments and other conditions that can affect the outcome. This is generally true of any analytical method that employs solutions to differential equations as the basis of the predictions. We will show how to solve the differential equations describing molecular mass diffusion in polymers, and the chemical reactions in the material that can give rise to performance changes in materials within the finite element (FE) method. We limit our interest to the processes of material aging caused by diffusion and (chemical) reaction (DR) processes only. Once the FE method for the treatment of these specific processes is established, it would be possible to extend the method to include other processes if they are expressed appropriately in the governing equations and any constitutive relationships are posed or expressed. Additionally, the FE method usually models physical situations where gradients of some state or property are expected to be present, such as gradients in temperature or displacements. In our case, we will see that we would expect to have gradients in the concentration of chemical species in the applications of interest.

Finally, we are motivated to use the FE method, not only because of its widespread use in practice, but because we ultimately wish to apply the results of an aging analysis in a structural (solid mechanics) or failure analysis using the same analysis method. Commonality of the analysis method and code sharing is a key feature of this approach.

Mass Balance Equations

For a particular mobile chemical species, the ith species, in a mixture of n chemical species $1, \ldots, i, \ldots n$, such as a polymer, the governing equations for mass balance for species i is given by[8]

$$\frac{\partial C_i}{\partial t} = (\nabla \cdot D_i \nabla C_i) + R_i \tag{1}$$

The assumptions applicable to Eq. (1) are as follows:

1) Species i concentration in the mixture is dilute. (This implies the body does not change dimensions during diffusion and reaction, i.e., it does not shrink or swell.)

2) The DR processes are isothermal.

3) No convection of mass occurs.

There are n mass balance equations, one for each of the n chemical species in the mixture. We will assume the diffusivity of species i can be a function of C_i but not $C_j (i \neq j)$ or any of the other j species. This decouples the n equations through the diffusivity coefficients. However, coupling of the equations can occur through the chemical reaction term R_i.

A fundamental assumption of the FE method is that the solution variable is continuous in the computation domain, specifically the displacement vector $\boldsymbol{u}$ for solid mechanics and the temperature vector $\boldsymbol{T}$ for heat conduction. However, a chemical species can be discontinuous across a material boundary, where the solubility of the species is different in the two or more materials. Because concentration is the solution variable in the mass balance equation, we can modify Eq. (1) to replace C_i with another dependent variable chosen to be continuous across material interfaces and, thus, conform with the FE method's requirement of a continuous solution variable in the computational domain. Although Eq. (1) can be solved by various methods other than the FE method, the modification of Eq. (1) to a continuous solution variable is necessary to solve it via the FE method.

Henry's Law

We can assume that the aging rates of change are slow, taking days and even years to occur. We can then look to equilibrium thermodynamics to choose an appropriate constitutive relationship to modify the governing equations. We can use Henry's law (see Ref. 9) of solubility:

$$C_i = S_i p_i \tag{2}$$

The use of this relationship presumes that each of the n chemical species in the mixture is gaseous, has a vapor pressure, and can dissolve in the mixture. Because S_i is specific to a material, we choose p_i, the species partial pressure, to be continuous across a material interface, which will replace C_i as the solution variable in Eq. (1). The use of Henry's law presumes that p_i exists in the solid material. Physically, this may or may not be true, but we choose to use p_i as a convenience to solve Eq. (4) in the FE method context. Note that p_i is usually very small. (S_i commonly have very large values.) We should not confuse p_i with a potentially larger normal pressure (the diagonal entries in a stress tensor) experienced in a solid mechanics situation. Hence, the assumption is that if p_i exists, it does not significantly contribute to a material's stress state.

We substitute Henry's law into Eq. (1) and make the partial pressure p_i the new solution variable. This is the first key concept in our development of the method. The approach is to solve the governing equations for p_i for all time in the domain via the FE method and subsequently to convert the partial pressures back to concentrations C_i using Henry's law.

Analogy to Heat Conduction

The second key concept is that, by inspection, Eq. (1) for is analogous in form to the governing equation for heat conduction[8]

$$\rho C_p \frac{\partial T}{\partial t} = \nabla \cdot \nabla(\kappa T) + \Phi \tag{3}$$

We can compare the heat conduction equation to the modified mass balance after substitution of Henry's law:

$$\frac{\partial (S_i p_i)}{\partial t} = \nabla \cdot \nabla(D_i S_i p_i) + R_i \tag{4}$$

The functional forms of the two governing equations are identical, except that the mass balance is a system of n equations, and there is only one energy balance equation per material. The coefficients are analogous as well: S is the mass solubility analogous to ρCp, the volumetric specific heat, and DS is the mass permeability, analogous to the heat conductivity. The source terms R_i and Φ are also analogous, representing the volumetric source of mass and heat, respectively. Because much of the FE literature is devoted to solving the heat conduction equation, we can leverage much of the prior computer code and architecture to our advantage in solving the DR equation system.

Boundary Conditions

Boundary conditions for Eq. (4) are also analogous to heat conduction with the exception of surface radiation of energy to an external environment, which does not have an analog in mass transport. We specify partial pressure of species i at an external boundary (Dirichlet condition), a mass flux of species i at an external boundary (Neumann condition), and a "mixed" flux condition, where a film mass transfer coefficient h is defined. Note that, if no boundary condition is specified, the default condition is $\boldsymbol{j}_i = 0$ through the boundary (no flux).

Chemical Reactions

The unique feature of the DR equation system is the general functional form of the chemical rate (kinetic) expressions and that the reaction expressions couple some or all of the n mass balance equations. We consider only homogeneous reactions occurring in the volume of the body or the element. Typically, classical chemical kinetics expressions of continuum materials are posed as polynomials, depending on the chemical reaction postulated for any given application. We can choose the kinetic rate form for species i:

$$R_i \frac{\mathrm{d}C_i}{\mathrm{d}t} = \sum_{j=1}^{m} k_j \left[\prod_{r=1}^{s} C_r^n \right] \tag{5}$$

The n in Eq. (5) are not restricted to integers but may be real numbers. We have departed from the more formal definitions of chemical rate[10–12] to make the kinetic forms completely general and not be restricted to any specific chemical reaction rate expression. The form of the rate expression (5) is not unique; we could have chosen, from many polynomial forms, smooth functions within the intervals of species concentrations desired.

FE Architecture

We apply the Galerkin approach (see Refs. 13 and 14) to Eq. (4), using solid element formulations commonly used for heat conduction. We will omit the details, suffice to say that it parallels the development of the heat conduction equations in FE. See Ref. 15 for a complete description of the DR FE equations and discretization.

Because there are n governing equations for DR, the forms of the solution vector and other vectors/matrices must accommodate this feature. We adopt a convention that number the species in a user-defined order; thus for isothermal situations, the partial pressure solution vector has the form

$$\boldsymbol{p} = \begin{bmatrix} p_{\text{species 1}} \\ p_{\text{species 2}} \\ \bullet \\ p_{\text{species } n} \end{bmatrix} \Big\rangle \text{node 1} \quad \begin{bmatrix} \boldsymbol{p} \\ \boldsymbol{p} \\ \bullet \\ \bullet \\ \bullet \\ \boldsymbol{p}_{Nel\ \text{nodes}} \end{bmatrix} \begin{matrix} \rangle \text{node 2} \\ \rangle \text{node 3} \end{matrix} \tag{6}$$

The stiffness and capacitance matrices follow forms similar to heat conduction for a one-dimensional linear two-node bar element.

FE Solution Behavior

We can test the FE solutions of DR against those of exact solutions for situations of one-dimensional, steady-state, and transient response. An example is given to demonstrate general behavior of the diffusion FE solution for adjacent materials of differing solubilities.

One-Dimensional, One Species, Two Materials, Transient Diffusion (No Chemical Reaction)

We pose this case to demonstrate the ability of the FE solution to partition correctly unequal concentrations across material boundaries due to unequal material solubilities. We model the process using a multiple-element one-dimensional FE model, to capture the concentration gradients developed by the diffusion process. The model is shown in Fig. 1, where material 1 is the interval $w \le x \le 0$ and material 2 is interval $0 \le x \le L$. The diffusivities and solubilities are chosen to generate spatial gradients and concentration step at $x = 0$. C_L is the left-hand boundary condition, a constant concentration. The right-hand boundary condition is a zero mass flux condition. The initial condition C_0 is assumed zero in both materials for all x. The exact solution (personal communication from I. L. Davis, Thiokol Corp., Brigham City, Utah, 1999) for material 1 can be shown to be

$$C(x,t) = C_0 + \sum_{n=1}^{\infty} B_n \cos(\lambda_n L) \sin[k\lambda_n(x+w)] e^{-\lambda_n^2 D_1 t} \qquad (7)$$

for $w \le x \le 0$ and $t > 0$. The solution for concentration for material 2 can be shown to be

$$C(x,t) = \frac{S_2}{S_1} C_0 + \frac{S_2}{S_1} \sum_{n=1}^{\infty} B_n \sin\left(\lambda_n w \sqrt{\frac{D_2}{D_1}}\right) \cos[\lambda_n (x-L)] e^{-\lambda_n^2 D_2 t} \qquad (8)$$

for $0 \le x \le L$ and $t > 0$. Here the coefficients B_n are computed by

$$B_n = \frac{-2C_0 \cos(\lambda_n L)}{k\lambda_n [w \cos(\lambda_n L) + (S_2/S_1) L \sin(k\lambda_n w)]} \qquad (9)$$

and the eigenvalues λ_n are computed by

$$\tan(\lambda_n L) \tan(k\lambda_n w) = 1/[k(S_2/S_1)] \qquad (10)$$

The preceding solutions for specific cases are obtained by means of a FORTRAN computer code. The FE model is constructed with 10 one-dimensional linear (bar) elements in each material and according to the illustrated configuration. Time is integrated using the Crank–Nicholson method for times of $1E6$, $1E7$, $1E8$, $1E9$, and $1E10$, providing a span of concentration profiles. These times are generic for this model and are indicative of a very slow diffusion process. The FE and exact solutions are plotted in Fig. 2 for equal solubilities in materials 1 and 2, and the material interface is at $x = 0$.

More illustrative is the solution for unequal lengths, diffusivities and solubilities: $D_1/D_2 = 0.1$, $S_1/S_2 = 0.1$, and $L_1/L_2 = 0.1$ in Fig. 3. The concentration discontinuity is clear in this example, showing a comparison of exact and FE solutions. There are endless combinations of solubilities, diffusivities, and lengths possible, all with similar results. This is presented as an example and not as a general result, although it is possible to nondimensionalize the exact solution and make general comparisons with the FE solutions.

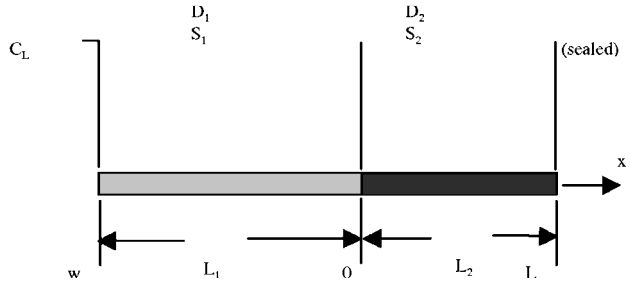

Fig. 1 One-dimensional FE model, two materials.

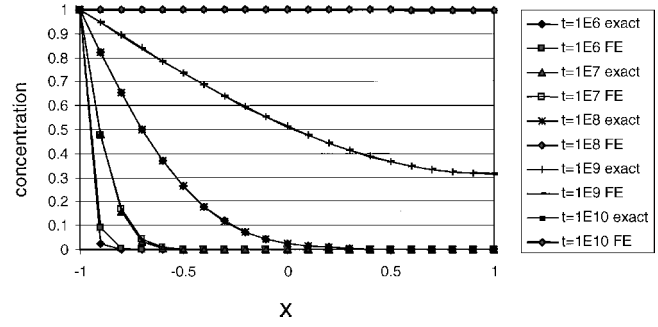

Fig. 2 Linear diffusion FE vs exact solution, equal solubilities.

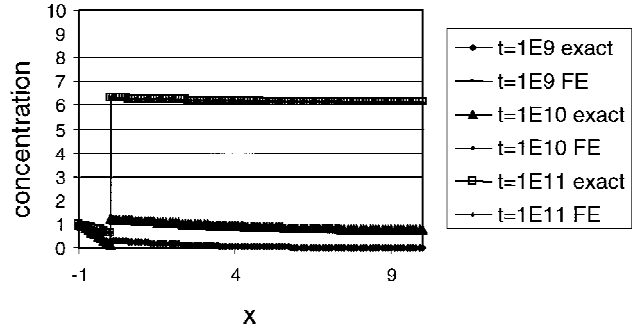

Fig. 3 Linear diffusion FE vs exact solution, unequal solubilities.

Nonisothermal FE Architecture

Varying temperature can also be solved by an extension of the given architecture. Because the standard heat conduction governing equation is of the same form and analogous in behavior to the DR equations, we simply add temperature to the solution vector, in the first position in the solution vector:

$$\boldsymbol{p} = \begin{bmatrix} T \\ p_{\text{species 1}} \\ \vdots \\ p_{\text{species } n} \end{bmatrix} \text{node 1} \quad \begin{bmatrix} T \\ \boldsymbol{p} \end{bmatrix} \text{node 2} \quad \begin{bmatrix} T \\ \boldsymbol{p} \end{bmatrix} \text{node 3} \quad \vdots \quad \begin{bmatrix} T \\ \boldsymbol{p} \end{bmatrix} Nel \text{ nodes} \qquad (11)$$

One must exercise care in constructing the stiffness and capacitance matrices to separate the thermal material properties and the DR properties. To illustrate, we choose the one-dimensional linear bar element with the following shape function $N(x)$:

$$\boldsymbol{N}(x) = [1 - x/L, 1 - x/L, x/L, x/L] \qquad (12)$$

The element stiffness matrix for temperature and a single chemical species is

$$\boldsymbol{K} = \frac{A}{L^2} \begin{bmatrix} \kappa & 0 & -\kappa & 0 \\ 0 & SD & 0 & -SD \\ -\kappa & 0 & -\kappa & 0 \\ 0 & -SD & 0 & SD \end{bmatrix} \qquad (13)$$

where the separation of thermal and mass transport properties is evident. The consistent capacitance matrix is

$$\boldsymbol{C} = \frac{AL}{6}\begin{bmatrix} 2\kappa & 0 & \kappa & 0 \\ 0 & 2S & 0 & S \\ \kappa & 0 & 2\kappa & 0 \\ 0 & S & 0 & 2S \end{bmatrix} \tag{14}$$

DR and Thermal Coupling

If the rates of heat conduction and the rate of diffusion and/or the rate of chemical reaction are nearly the same, then the equations need to be solved simultaneously. We need a constitutive relationship between the DR material properties and the thermal state variables to determine the coupling. For many polymers, the Arrhenius relations are a good means of expressing these relationships:

$$D = D_0 \exp(-E_d/RT), \qquad k = k_0 \exp(-E_r/RT)$$
$$S = S_0 \exp(-E_s/RT) \tag{15}$$

Typically, polymer-solutes display diffusion activation energies about 10–20 kcal/g · mol, and roughly the same order of magnitude for solubility (except negative). Reaction rate constant activation energies can be anywhere from 10 to 40 (or larger) kcal/g · mol, for example, see Ref. 16. The sensitivity of diffusivity, solubility, and rate constant are typically larger than the sensitivity of density, specific heat, and/or thermal conductivity to temperature, and so we can ignore the nonlinear effect of temperature-dependent thermal properties in temperature ranges where the DR properties would show significant sensitivity. Thus, typically, the coupling is from the thermal to the DR equations through the temperature. In this case, we can pose the stiffness and consistent capacitance element matrices, respectively, for the one-dimensional linear element, as before:

$$\boldsymbol{K} = \frac{A}{L^2}\begin{Bmatrix} \kappa & 0 & -\kappa & 0 \\ 0 & S_0 D_0 \exp[-(E_D + E_S)/RT] & 0 & -S_0 D_0 \exp[-(E_D + E_S)/RT] \\ -\kappa & 0 & -\kappa & 0 \\ 0 & -S_0 D_0 \exp[-(E_D + E_S)/RT] & 0 & S_0 D_0[-(E_D + E_S)/RT] \end{Bmatrix} \tag{16}$$

$$\boldsymbol{C} = \frac{AL}{6}\begin{bmatrix} 2\kappa & 0 & \kappa & 0 \\ 0 & 2S_0 \exp(-E_S/RT) & 0 & S_0 \exp(-E_S/RT) \\ \kappa & 0 & 2\kappa & 0 \\ 0 & S_0 \exp(-E_S/RT) & 0 & 2S_0 \exp(-E_S/RT) \end{bmatrix} \tag{17}$$

The preceding description relates to the fully coupled DR and thermal systems of equations. Clearly, within the same FE code one can treat uncoupled DR and thermal response when the DR rates of change are typically very much slower than heat conduction. In this situation, the user simply needs to solve the heat conduction problem for the body and time span of interest, save the results, and conduct a separate DR analysis. The temperatures from the saved thermal analyses are read in and applied as the means of modifying the appropriate material parameters or environmental loads.

Application of the Method

We now describe an application of the method, with comparisons of model predictions of chemical species concentrations compared to aging data. Of interest is a large cylindrical solid body (an "asset") constructed of multiple layers of different polymeric materials through which identifiable chemical species can diffuse and react. The two assets described in this paper were taken from a population of assets of the same design and manufacturing process, but of different ages, and from different lots of raw materials. From studies conducted by the U.S. Navy, the important soluble mobile chemical species are well known, as well as the dominant chemical reactions occurring in the materials of interest. It is already known that all assets of the population exhibit the same characteristic chemical aging changes. The asset dimension of interest is on the order of a meter to several meters in diameter, and the asset typically weighs several metric tons.

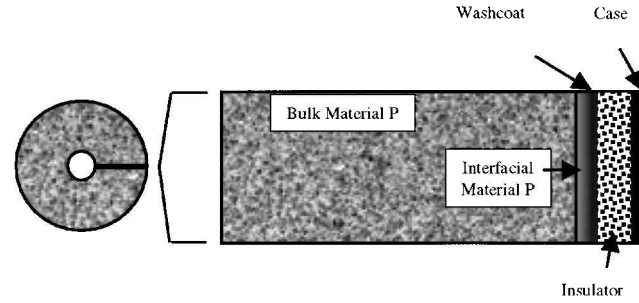

Fig. 4 Asset geometry (not to scale).

A simplified illustration of the asset is shown in Fig. 4, made up of a shell of fiber composite (case) with a layer of polymeric rubber (the insulator, or material I) inside and vulcanized together. A liner of curable polymeric liquid (washcoat) is subsequently applied to the inside of the insulator, and the empty built-up case is cast with a curable slurry of polymeric binder and powdered solids, which is designated material P. The assembly is cured at an elevated temperature, at about 130°F, to solidify (chemically cross link) the material P binder. The asset is then subjected to finishing operations and kept within relatively narrowly controlled temperature limits. For the purpose of this study, the asset temperature is assumed to be at a constant and uniform 77°F throughout its life.

Material P contains mobile species within the polymeric binder, which are soluble in the liner, insulator, and case. During the cure cycle, these chemical species diffuse into these adjacent materials and can also chemically react. After curing, the mobile species continue to diffuse into the adjacent materials throughout the useful life of an asset, although more slowly at the relatively lower use temperature. The concentration of the chemical species in the asset during its entire lifetime is of primary interest because the levels can be used to define the service lifetime of the asset.

During the manufacturing process where an uncured liquid polymeric slurry of material P exists and after cure and during service, these species will diffuse across the washcoat (also known as the P/I interface) and create concentration gradients in the radial direction in adjacent materials near this interface. This diffusion reduces the concentration of each of the species in the bulk material P at the P/I interface. The concentration loss is partially compensated by diffusion of material from the bulk material P into the interface region. The diffusion creates a spatial profile of the mobile species near the P/I interface that changes over time as the diffusion and reactive processes proceed.

Modeling Approach

The intent is to demonstrate that the diffusion-reaction model can reproduce the chemical concentration gradients near a material interface and, therefore, can represent the dominant process controlling the chemical gradients over time.

The DIAL©[17] FE code was used to model the effect of chemical reactions and mass transport on the evolution of these concentration profiles. We will use gradients determined from samples dissected and extracted from assets to compare to the FE model predicted

gradients. Because we have assets of various ages, we can attempt to match predicted and observed chemical gradients over a period of time, as represented by sample snapshots. However, the number of assets available for sampling and testing is limited to only a handful, and meaningful statistical treatment of the observed data is not possible. The goal of this data fitting process is to determine the features, properties, and load inputs to the FE model that can match gradients from assets of all ages. This process is much the same as fitting an analytic function to data by a least-squares process. However, in this case, the function that we use to fit the data is the DR FE solutions. With this fitting accomplished, subsequent predictions of chemical profiles can be made beyond the existing data sets. In this study, we will limit the exploration of the data to the model fitting process.

Because only the asset center bore (element on the extreme left) and external case surface (element on the extreme right) are exposed to the external vapor environments, we need to ascribe boundary conditions only to these element nodes. The "cut" element surfaces through the asset are not subject to significant gradients (the z direction along the cylinder axis) and the θ (tangential) direction, and, therefore, the default boundary conditions, with no mass flux, are used. Grid spacing in the bulk of material P is fine in the interface areas, anticipating the need to capture the expected concentration gradients in these areas; we anticipate concentration gradients only in the radial direction in the assets and only significantly near the P/I interface, where concentrations of the species of interest are significantly different at time zero in adjacent materials.

We postulate the dominant chemical reactions that represent test observations and provide the parameters that describe the chemical reaction rate constants and initial concentrations in each of the materials in the application, as well as the diffusional mass transport described by the diffusion and solubility coefficients. These initial parameter sets were derived from data collected from subscale studies. Once these parameter sets have been defined, the partial pressure solutions as a function of time are determined by an appropriate time-stepping algorithm in the FE code, using the Crank–Nicholson time-stepping algorithm. The Crank–Nicholson algorithm is used for all applications because of its optimal accuracy and unconditional stability. The partial pressure solutions, saved at user defined time-step intervals, are converted to species concentrations by recovering the user specified solubility of each element and the appropriate use of Henry's law.

The FE computed species concentration radial profiles are compared to concentration profile data taken from relatively new and old assets subjected to destructive sampling, dissection, and subsequent testing. Care is taken in the construction of the FE grids to ensure that an element is approximately centered at the same radial location as each of the data locations. There are always instances where there are more model elements than data locations, but never less.

The species concentration data[18] are determined by solvent extracting small weighted samples from the asset dissection (a layered dissection pattern to discern the expected radial concentration profile) and subjecting the extracts to high-performance liquid chromatography (HPLC). When compared to known standards analyzed by the same method, the concentrations of the mobile species are determined. The measured concentration profiles are then compared to the computed profiles, and in an iterative fashion, we converge on a model-input parameter set that best fits the sample observations. The best-fit input set is compared to existing material properties to ensure the model material properties are consistent with independently determined values. No quantitative means were employed to iterate to a best fit to the data, rather, the results of each iteration of data fitting process was reviewed by a committee to guide and control the model changes. This process was conducted in this manner in part as a learning experience to ensure consistency with data and evidence from prior work.

The primary chemical species, which we name NP, MA, NDPA and NOMA, are present only in the material P binder at time zero, the time before elevated temperature cure. NP is a mobile plasticizer soluble in the material P binder that can undergo a spontaneous decomposition into smaller molecules. MA is in relatively smaller concentration than NP at zero time and acts to scavenge NP decomposition products, primarily NO_2 in the binder created from the NP decomposition. If the NO_2 were not removed, it is highly reactive and can promote further decomposition of the NP. The species NOMA is the reaction product of MA and NO_2, which is known to be relatively unreactive with the other species present in material P binder. NOMA is also relatively stable and does not spontaneously decompose. NDPA is a secondary NO_2 scavenging species formulated into material P that can also react with NO_2, but at a measured rate much slower than MA.

Material P contains dispersed solids suspended in a polymeric binder. The dispersed solids are known not to contribute to the NP or MA chemical reaction processes and, for purposes of aging behavior, are considered inert. The FE method uses continuum-based material properties, and because the mean diameter of the dispersed solids in material P is very much smaller than the linear dimension of the smallest element of the model, all species concentrations are based on the content of the species in the continuum of binder and solids mixture. Thus, the diffusion and reaction properties are determined to reflect the mixture of reactive and inert materials in material P.

Equation (18) is a list of the dominant chemical reactions postulated to occur in material P. The notion is to keep the kinetic rate equations as few and as simple as possible and to add complexity only when needed to resolve discrepancies with observations. Reaction products known to be relatively unimportant to the primary aging process are listed as products, thus,

$$\mathrm{NP} -> \mathrm{NO_2} + (\text{products}), \qquad \mathrm{NO_2} + \mathrm{MA} -> \mathrm{NOMA} \tag{18}$$

The losses of NP and MA due to chemical reactions are described by a set of first-order (in time) differential rate equations. The reaction orders are all assumed first order in each chemical species appearing in the rate expressions. The rates are expressed as uniformly distributed in a volume (element). The postulated kinetic rate expressions for NP, MA, and NOMA are given by

$$\begin{aligned}
\frac{\mathrm{d}C_{\mathrm{NP}}}{\mathrm{d}t} &= -k_{\mathrm{NP}}C_{\mathrm{NP}} \\
\frac{\mathrm{d}C_{\mathrm{NO2}}}{\mathrm{d}t} &= k'_{\mathrm{NO2}}C_{\mathrm{NP}} - k''_{\mathrm{NO2}}C_{\mathrm{NO2}}C_{\mathrm{MA}} \\
\frac{\mathrm{d}C_{\mathrm{MA}}}{\mathrm{d}t} &= -k_{\mathrm{MA}}C_{\mathrm{NO2}}C_{\mathrm{MA}} \\
\frac{\mathrm{d}C_{\mathrm{NOMA}}}{\mathrm{d}t} &= k_{\mathrm{NOMA}}C_{\mathrm{NO2}}C_{\mathrm{MA}}
\end{aligned} \tag{19}$$

The reaction rate constants employed for the two chemical reactions in each of the materials are detailed in Ref. 15.

Material Properties

The diffusion and solubility coefficients employed for all of the molecular species in each of the materials are listed in Ref. 15 and were derived from subscale test articles using a variety of different concentrations of NP, MA, NDPA, and NOMA. These tests were designed and conducted such that one-dimensional concentration profiles of these species were developed from the application of uncured binder on a single surface of the sample. The other surfaces were sealed with impermeable coating such that no significant mass transport would occur and affect the concentration profiles developed in anticipated areas. The cartons were maintained at constant temperatures for various periods of time and periodically withdrawn, dissected, and tested to measure the concentration profiles by HPLC. Simple one-dimensional FE diffusion models were constructed, and the diffusivities of each of the species were determined by a least-squares best fit of the predicted profiles to the profile data. Within the period of these tests, and at the relatively low temperatures used, no significant chemical reactions occurred that would confound the determination of the diffusion coefficients.

Model Assumptions

In the development of the model, certain parameter values had to be estimated because experimental data are unavailable. In addition, observations from the asset sample data permit us to make additional

conclusions or assumptions. The assumptions made in this model are based on historical observations:

1) The observed NOMA concentration at any given location in material P vs time show a nonzero intercept with asset age; therefore, formation of NOMA is believed to occur during the curing process and must be accounted for.

2) The NOMA concentration profiles show a maximum value near the P/I interface, and we have concluded the reaction rate constants are higher in insulator than in the bulk material P.

3) For a given asset age, the highest observed NOMA concentration appears in interfacial material P adjacent to thick material I; therefore, we have concluded there is a material I thickness hbox dependence.

4) The same chemical reactions take place in adjacent materials and are expressed by the rates given earlier and have the same rate constants.

5) There is species molar balance: For every mole of NO_2 produced, one mole of NP and MA is consumed and one mole of NOMA is produced.

6) The relative solubility of all mobile species in material I is less than in bulk material P.

7) Interfacial material P (the region within 1–2 mm of the interface) appears different from bulk material P: We have assumed the existence of a solubility gradient, probably resulting from the cure process.

8) The steady-state NO_2 concentration in bulk material P is approximately 1 ppm. NO_2 concentration cannot be directly measured in material P by any means known.

9) The relative solubility of all species in all materials during cure is the same as that during aging.

Boundary Conditions

All chemical species in this FE model are known to be volatile, having a small, but finite vapor pressure. These species are not normally present in ambient air, and the assets are normally stored in conditions where free air exchange is the norm. Fixed zero concentration (partial pressure) nodal loads are applied to nodes located at model boundaries adjacent to external environments. Default (no-flux) boundary conditions are assumed at all model internal element faces.

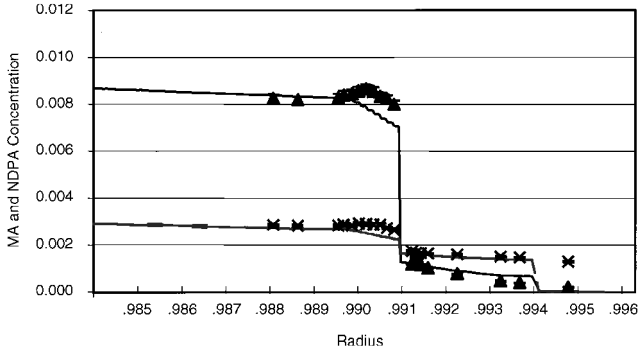

Fig. 5 NP concentration vs asset radius for asset 1, one year.

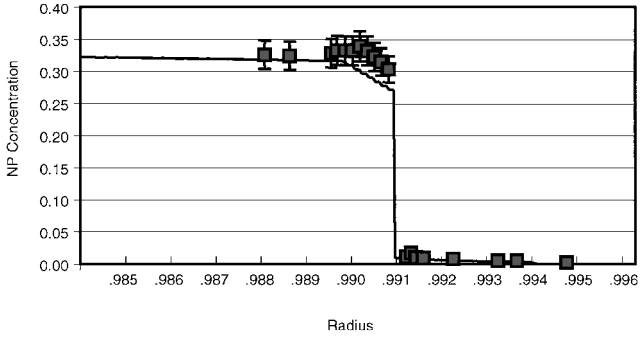

Fig. 6 MA (upper curve) and NDPA concentration vs radius (lower curve) for asset 1, one year.

Results Summary

The concentration profile data for NP, MA, NDPA, and NOMA from the available asset sample data were analyzed for initial estimates of chemical rates. The objective of the analysis was to estimate the bulk material P reaction rates during the cure and aging process for use in the FE model. For the cure process, we have assumed a temperature of 130°F and a cure time of approximately one week, typical for asset production cycles. The loss rate of NP and MA in bulk material P during cure is on the order of 10^{-4} and 10^{-5} g/cm^3 · day, respectively. These rates were calculated by plotting the NOMA concentration as a function of time in earlier studies. The intercept of the line determines the amount of NOMA formed during cure, and the slope determines the amount formed during aging. These values served as the initial starting point for the reaction rate constants and initial conditions.

Asset Sample Data

The asset sample data that were available during this time period are tabulated in Ref. 15. Several data sets were available for each asset. Some of the samples extracted from the available assets have varying insulator thickness, which must be accounted for in the models because chemical gradients are created in this material, and their presence also affects the creation of gradients in adjacent materials.

Figures 5–10 show the comparisons of the FE models (distinct models for each asset) with the appropriate asset sample concentration data. Figures 5–10 focus on the material interface region of the assets tested, rather than the entire profile because the region of concentration gradients is observed to occur only in this region.

Typical Results

Figures 5–10 are comparisons of the computed and experimental concentration profiles for assets 1 and 2 tested for mobile species profiles. Motor radii in Figs. 5–10 are normalized. Asset 1 was 1 year old and asset 2 was 10.6 years old when sampled. In all cases shown, the profile data error bars represent ±1 standard deviation from replicate tests, and the solid line represents the FE model prediction. All prediction-data fit errors were less than ±5%.

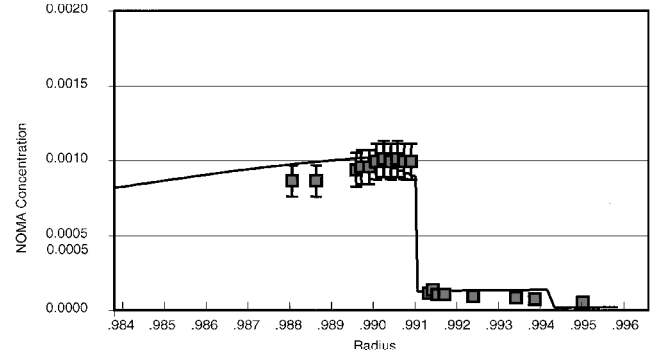

Fig. 7 NOMA concentration vs radius for asset 1, one year.

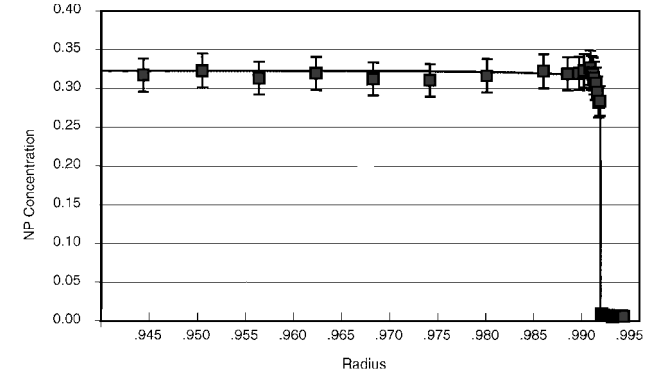

Fig. 8 NP concentration vs radius for asset 2, 10.6 years.

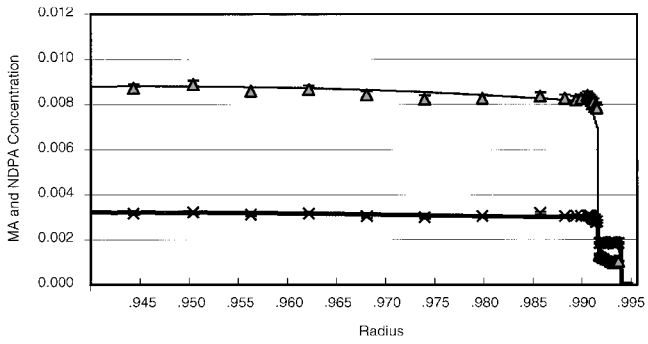

Fig. 9 MA (upper curve) and NDPA (lower curve) vs radius for asset 2, 10.6 years.

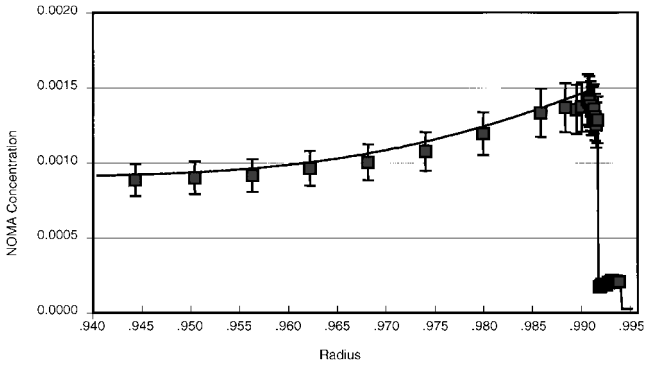

Fig. 10 NOMA concentration vs radius for asset 2, 10.6 years.

Discussion

The model predicted concentrations for both the 1- and 10.6-year-old assets show a relatively good fit to the data, mostly within the 1 standard deviation range. This is typical of other assets of similar ages. NO_2 concentration profiles are not plotted because it cannot be measured in these materials.

The trends of data and models are what we would anticipate of systems where NP, MA, and NDPA all deplete over time, and NOMA increases over time. NOMA also shows a peak in concentration that increases over time. Although counterintuitive, independent studies have shown that NOMA exhibits a higher production rate in the insulator adjacent to material P.

Note that the model for these two assets varied only in spatial dimensions of the materials because the two assets in this study were sampled at two different locations. The material radial dimensions vary somewhat along the length of the cylinder axis, as well as exhibiting some manufacturing variation in dimension as well. The material properties and boundary conditions were the same for both models.

Conclusions

Through the use of Henry's law, we have shown that the governing equations of multiple species in multiple materials can be made consistent with the requirement of the FE method for continuous solutions in the computational domain. The use of species partial pressures correctly treats the concentration partitioning at material interfaces. FE solutions are computed in terms of species partial pressures and then converted to concentrations in postprocessing after the FE solution(s) are determined at each time step.

The DR governing equations, after modification by Henry's law, are completely analogous to the heat conduction equation, except that there are n DR equations. We show the solutions to the isothermal steady-state solutions, and the transient solutions, are consistent with exact solutions. General one-dimensional behavior for DR solution accuracy can be established for linear and quadratic solid bar elements.

A secondary outcome of this method is that the FE architecture for solving the DR equations can be easily expanded to nonisothermal problems of DR, either serially (uncoupled) or fully coupled. The comparisons to aging data, although showing some variation in the goodness of fit, are consistent for asset to asset, over a range of asset age. Most of the comparisons of model to data show the predictions fall within the $pm1$ data standard deviation range. Further refinement of model inputs only manipulates the predicted concentration within these data variation bands, which does nothing to increase confidence in the model fit to the data. Because the models used only one set of material properties and boundary conditions, we can confidently claim that the model should correctly predict future trends in the concentration of these species.

References

[1] Struik, L. C. E., *Physical Aging of Amorphous Polymers and Other Materials*, McGraw–Hill, New York, 1978, pp. 28–35.

[2] Viebke, J., and Gedde, U. W., "Antioxidant Diffusion in Polyethylene Hot Water Pipes," *Polymer Engineering and Science*, Vol. 37, No. 5, 1997, p. 896.

[3] Hogan, D. K, *Proceedings of the Joint Army Navy NASA Air Force Structures and Mechanical Behavior Subcommittee*, Dec. 1996.

[4] Mastin, L. A., *Proceedings of the Joint Army Navy NASA Air Force Structures and Mechanical Behavior Subcommittee*, Dec. 1997.

[5] Fisher, J. M., *Proceedings of the Joint Army Navy NASA Air Force Structures and Mechanical Behavior Subcommittee*, Dec. 1997.

[6] Culver, T., *Proceedings of the Joint Army Navy NASA Air Force Structures and Mechanical Behavior Subcommittee*, Dec. 1997.

[7] Herring, E. J., and Carden, J. P., "Aging Behavior of Composite Solid Rocket Motor Bondlines," *Proceedings of the Joint Army Navy NASA Air Force Structures and Mechanical Behavior Subcommittee*, New Orleans, LA, Nov. 1992.

[8] Byrd, R. B., Stewart, W. E., and Lightfoot, E. N., *Transport Phenomena*, Wiley, New York, 1960, pp. 502, 503, 566.

[9] Denbigh, K., *The Principles of Chemical Equilibrium*, 2nd ed., Cambridge Univ. Press, Cambridge, England, U.K., 1968, pp. 264–267, 281, 282.

[10] Mahan, B. H., *University Chemistry*, 2nd ed., Addison Westly Longman, Reading, MA, 1969, pp. 354–373.

[11] Atkins, P. W., *Physical Chemistry*, Q. H. Freeman, 1978, p. 86.

[12] Glasstone, S., *Thermodynamics for Chemists*, D. Van Nostrand, 1947, pp. 105–107.

[13] Hughes, T. J. R., *Finite Element Method*, Wiley, New York, 1992, pp. 50–54.

[14] Bathe, K. J., *Finite Element Procedures*, Prentice–Hall, Upper Saddle River, NJ, 1996, pp. 538, 539.

[15] Wadiak, D. T., "Diffusion and Chemical Reaction by the Finite Element Method," Ph.D. Dissertation, Dept. of Mechanical Engineering, Santa Clara Univ., Santa Clara, CA, June 2002.

[16] Hamid, S. H., Amin, M. B., and Maadhah, A. E., *Handbook of Polymer Degradation*, Marcel Dekker, New York, 1992, pp. 205, 206.

[17] "The Lockheed Martin DIAL© Finite Element System," Ver. L3D5, Lockheed Martin Space Systems Co., Sunnyvale, CA, Sept. 2002.

[18] Sinclair, J., *Proceedings of the Joint Army Navy NASA Air Force Structures and Mechanical Behavior Subcommittee*, Oct. 1998.

T. C. Lin
Associate Editor